

An assessment of NSCAT ambiguity removal

Amy E. Gonzales and David G. Long

Department of Electrical and Computer Engineering, Brigham Young University, Provo, Utah

Abstract. The NASA scatterometer (NSCAT) estimates the wind speed and direction of near-surface ocean wind. Several possible wind vectors (termed ambiguities) are estimated for each resolution element known as a wind vector cell (WVC). Typically, the speeds of the possible wind vectors are nearly the same, but the directions are very different. The correct wind must be distinguished in a step called ambiguity removal. Unfortunately, ambiguity removal algorithms are subject to error. In an attempt to evaluate the accuracy of the Jet Propulsion Laboratory NSCAT product, we use a new model-based quality assurance algorithm that uses only NSCAT data. The algorithm segments the swath into overlapping 12×12 WVC regions and classifies each region according to estimated quality. The 9-month NSCAT mission data set is analyzed. In 82% of the regions the ambiguity removal is over 99% effective, with the ambiguity errors correctable using a model-based correction technique. In 5% of the regions, areas of significant ambiguity error are found. For remaining regions, all of which have root-mean-square (rms) wind speeds less than 4 m s^{-1} , there is too much uncertainty in the wind field model or too much noise in the measurements to uniquely evaluate ambiguity selection with sufficient confidence. We thus conservatively conclude that for the set of regions with rms wind speed greater than 4 m s^{-1} , NSCAT ambiguity removal is at least 95% effective.

1. Introduction

Scatterometers do not directly measure the wind; rather, the speed and direction of the near-surface wind are inferred from the normalized radar cross-section (σ^0) measurements of the ocean surface. The wind is related to σ^0 via a geophysical model function. However, given the scatterometer measurements at an observation point or wind vector cell (WVC), there are several possible wind vectors for any particular set of σ^0 measurements [Long and Mendel, 1991]. Although the speeds are very similar, the directions vary with two to four possible directions for each WVC. Traditional pointwise wind retrieval consists of two steps and uses only the σ^0 measurements for a single WVC to retrieve the wind for that cell. The first step is to find the multiple wind vectors for each cell of the scatterometer swath. The second step, ambiguity removal, selects one unique wind vector estimate for each of these cells. Various ambiguity removal schemes have been developed [Schroeder *et al.*, 1985], including some fieldwise approaches [Hoffman, 1982; Atlas *et al.*, 1987]. For the NASA scatterometer (NSCAT) a modified median filter technique is used [Shaffer *et al.*, 1991; Shultz, 1990]. Correct ambiguity removal results in selection of the pointwise ambiguity that is closest to the actual wind vector. Unfortunately, ambiguity removal algorithms are prone to error. A quality assessment of these algorithms is essential to establish the integrity of the data.

A second method to determine wind estimates is model-based wind retrieval [Long, 1993]. The wind field model provides a description of the near-surface wind field over the scatterometer measurement swath and is optimized for scatterometer wind retrieval. The swath is sectioned into rectangular regions, and the wind is extracted over the entire region instead of by individual resolution elements. The model relates

the components of the wind vector field over this region to a set of model parameters [Long, 1993; Oliphant, 1996]. The models may be data driven or dynamics based.

The wind field models used in model-based wind retrieval can also be used to improve the pointwise wind product by identifying and correcting ambiguity removal errors. One way to do this is to fit the estimated pointwise wind to a simple wind field model over a small area. Since ambiguity removal errors typically cause 90° or 180° shifts in wind direction, large differences in the fit suggest possible ambiguity removal errors while small differences suggest a realistic or spatially consistent wind field. Ambiguity selection errors can be corrected by choosing the pointwise ambiguity closest to the model fit. This technique is exploited in the quality assurance (QA) algorithm that follows.

In this paper, a wind field model is developed and used to assess the accuracy of NSCAT ambiguity removal. A technique is then developed to detect and correct ambiguity removal errors using only NSCAT data. The results of using this technique on the data of the NSCAT mission (September 15, 1996 to June 29, 1997) are then presented. We conclude that NSCAT ambiguity removal is at least 95% effective for the entire set of regions with rms wind speeds greater than 4 m s^{-1} . This result is consistent with the comparisons with European Centre for Medium-Range Weather Forecasts (ECMWF) winds and buoy collocation statistics presented by Freilich and Dunbar [this issue] and Wentz and Smith [this issue].

2. Wind Field Model

The data used for the NSCAT ambiguity removal assessment are the NASA Jet Propulsion Laboratory (JPL) level 2.0 product for the NSCAT mission [Naderi *et al.*, 1991]. The wind resolution is 50 km. The Ku band NSCAT makes wind observations over a dual-sided swath that is 600 km wide or 12 WVCs on each side. Figure 1 is an example section of the

Copyright 1999 by the American Geophysical Union.

Paper number 98JC01943.
0148-0227/99/98JC-01943\$09.00

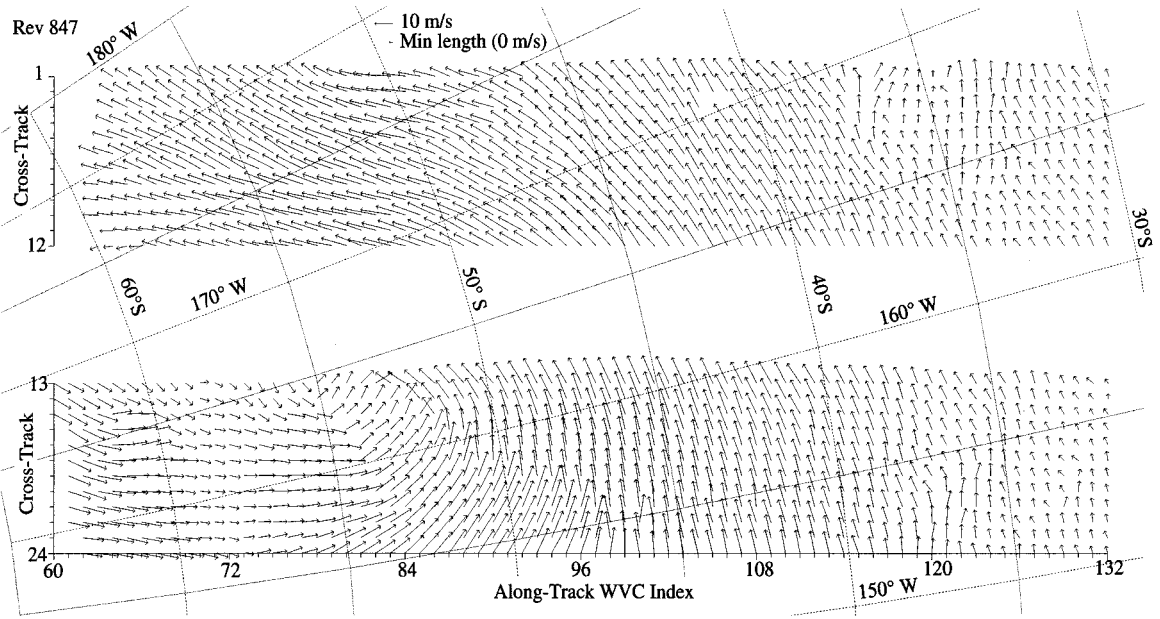


Figure 1. A sample wind field over the Pacific Ocean from the nudged Jet Propulsion Laboratory product for the ascending revolution number 847. A minimum vector length was used to clarify the presentation of very low wind speed vectors. WVC is wind vector cell.

observed wind field produced by JPL for ascending revolution 847. Two data sets (“nudged” and “unnudged”) were examined, each processed with the NSCAT 1 geophysical model function [Freilich and Dunbar, this issue; Wentz and Smith, this issue] which was tuned to NSCAT data. The same maximum likelihood wind retrieval technique is used for both data sets. The data contain up to four ambiguities per cell, ranked by likelihood with a flag to indicate the ambiguity selected by JPL. Pointwise ambiguity removal has been performed on the data using a median filter technique [Shaffer *et al.*, 1991; Shultz, 1990]. In median filtering, each swath is initialized separately by the most probable ambiguity for unnudged data and by global surface analysis fields from the National Center for Environmental Prediction (NCEP) for nudged data [Freilich and Dunbar, this issue]. In the nudged processing, data from NCEP are used to select which of the two most probable solutions are used to initialize the swath for implementing the median filter [Freilich and Dunbar, this issue]. The unnudged data exhibit more obvious ambiguity removal errors than nudged data.

2.1. Determination of the Model

As mentioned, wind field models can be used to assess the accuracy of ambiguity removal algorithms. In this work, a linear model similar to Long [1993] is used. It can be expressed as

$$\mathbf{W} = \mathbf{F}\mathbf{X}$$

where \mathbf{X} is an L element vector containing the model parameters and \mathbf{F} is a constant model matrix where the columns of \mathbf{F} form a basis set for possible wind fields. \mathbf{W} is a row scanned vector of winds sampled at the scatterometer observations over a small (12×12 WVC) region of the swath. For each 12×12 region, \mathbf{W} is defined in terms of the components of the wind:

$$\mathbf{W} = \begin{bmatrix} \mathbf{U} \\ \mathbf{V} \end{bmatrix} \quad (1)$$

where \mathbf{U} is a row-scanned version of the 12×12 matrix of east components of the wind and \mathbf{V} is a row-scanned version of the 12×12 matrix of north components of the wind. For both \mathbf{U} and \mathbf{V} the rows vary with cross track and the columns vary with along track.

Long [1993] used a simple dynamics-driven model for \mathbf{F} ; in this paper, we adopt a data-driven model matrix with a minimum number of basis vectors. We use the Karhunen-Loeve (KL) model since it is known to minimize the basis restriction error [Gunther and Long, 1994].

The KL model matrix \mathbf{F} is derived from the eigenvectors of the autocorrelation matrix \mathbf{R} of the sampled wind field [Gunther and Long, 1994]. \mathbf{R} is defined as $E[\mathbf{W}\mathbf{W}^T]$. Since \mathbf{R} is not known, it must be estimated from the sample autocorrelation. While a sample correlation could be computed from global circulation models (e.g., ECMWF or NCEP), these models are low resolution in comparison to the 50-km NSCAT resolution. Instead, the pointwise wind estimates from NSCAT data are used to compute an estimate of \mathbf{R} since we want to use only NSCAT data in the final analysis.

A portion of 3 weeks (128 revolutions) is used to estimate the sample autocorrelation. Each swath is segmented into 12×12 overlapping regions (approximately 53,000 regions), and \mathbf{W} is determined for each of the regions. An estimate of \mathbf{R} , R , is the sample average of the autocorrelation matrix

$$R = \frac{1}{N} \sum_{i=1}^N \mathbf{W}\mathbf{W}^T$$

where N is the number of regions.

Using standard eigenvalue/eigenvector decomposition methods, the model matrix \mathbf{F} is formed as the lower subset of the sorted eigenvectors of the sample autocorrelation matrix. The eigenvectors corresponding to the largest eigenvalues are the most important and are used as the columns of \mathbf{F} . Eigenvectors with very low eigenvalues describe wind field compo-

nents that are relatively rare or less important. Plots of the eigenvalues and the model-fit difference are useful for determining where to truncate the eigenvector series (see Figures 2 and 3). Visible in the eigenvalue plot, Figure 2, are some natural breakpoints, and the similarity between the unnudged and nudged data sets is apparent. Figure 3 shows the model-fit difference versus the number of basis vectors in the model. It was generated by fitting the model to nudged NSCAT data and calculating the vector rms difference. In this paper, the model matrix was subjectively chosen as the first 22 basis vectors of \mathbf{F} for the tradeoff between modeling error and the ability to locate regions with ambiguity removal errors. We note, however, that there is little performance difference in the QA algorithm when truncating the model between basis vectors 20 through 30.

2.2. Model Basis Vectors

We note that the truncated KL model is only minimally dependent on which data set is used to generate it, even though the unnudged winds contain many more ambiguity removal errors than the nudged data set. Separate KL models were computed for left and right swaths and both-nudged and unnudged JPL products. The low-order basis vectors are essentially identical for all cases. The basis vectors beyond the truncation point are the least important and have little effect on the truncated model. The truncated model admits basis vectors that describe the common wind fields that are essentially the same for nudged and unnudged data. Further, when the NSCAT WVC locations are used to sample ECMWF winds, the resulting KL model includes the similar low-order basis vectors, though the ordering is slightly different and the eigenvalues fall off more rapidly for higher-order vectors than with NSCAT winds. The latter can be expected since ECMWF winds are at lower resolution and thus are “low pass” compared with NSCAT winds. The robustness of the truncated KL model to the data set used to generate it suggests that the NSCAT winds are, on average, spatially self-consistent and that ambiguity removal errors (which, as noted later, affect less than 5% of the data) do not adversely affect the average low-order spectrum of the estimated winds. Thus the NSCAT-derived KL model can be used in evaluating ambiguity removal errors.

The truncated model is effective in spanning the majority of common wind fields since wind fields have a red power spectrum; that is the low-frequency components have the most energy. This is reflected in the KL model: low-order basis

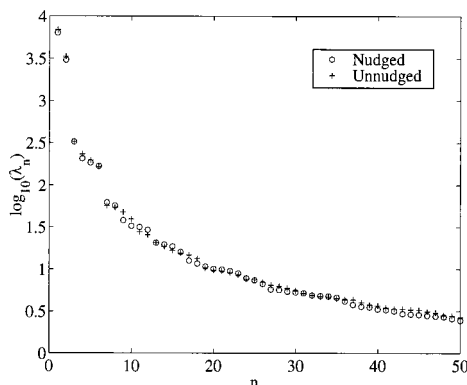


Figure 2. Eigenvalues of the sample autocorrelation matrix computed from 128 revolutions of nudged and unnudged data.

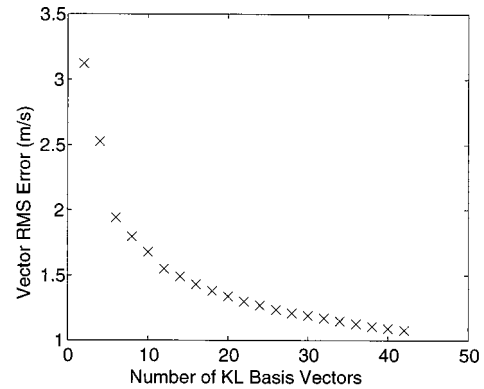


Figure 3. Vector rms error versus the number of Karhunen-Loeve model (KL) basis vectors (only even numbers shown) for the 128-revolution nudged test data set.

vectors exhibit only low-frequency components and have large associated eigenvalues compared with higher-order basis vectors which have smaller eigenvalues and higher-frequency components. If the entire KL matrix were used, any sampled wind field could be fit exactly to the model. However, by truncating the model, it can be used to identify regions of ambiguity removal errors since, while most realistic wind fields are spanned by the truncated model, fields with ambiguity removal errors are not.

The basis vectors corresponding to the first few eigenvalues are of interest as they mirror common natural wind fields. Figure 4 is a plot of the first six basis vectors for the KL model. The two most important basis vectors (i.e., those with the largest eigenvalues) correspond to the mean wind. The importance of these two basis vectors is evident from the large break in the eigenvalue plot between these and the subsequent eigenvalues. The next four are also representative of common wind patterns. The fourth and sixth are representative of cyclonic flows. The third and fifth are both examples of col points. As the eigenvalues for these wind fields suggest (Figure 2), these basis vectors are fundamental and are the bases for most wind fields.

Unfortunately, truncating the model does make some realistic wind fields inadmissible since not all real wind fields are adequately described by only the low-order basis vectors. This “modeling error” can be significant for some wind fields. As discussed in section 3.1, modeling error can be confused with ambiguity removal errors; this is a key limiting factor in our approach.

3. Methodology

To use the model as a quality assurance for the pointwise wind retrieval, the model is fit in a least squares sense to the observed pointwise wind field as described in this section. The swath is segmented into overlapping sections, and the model fit is tested for each section. The difference in the fit provides information about the “realism” of the observed wind. Thresholds are found for the model fit, and regions with statistics exceeding these thresholds are flagged as containing possible ambiguity removal errors. Corrections are then made when possible.

3.1. Using the Model Fit

A least squares estimate of the model parameter vector \mathbf{X} , $\hat{\mathbf{X}}$, can be obtained from the observed wind field \mathbf{W}_0 using the

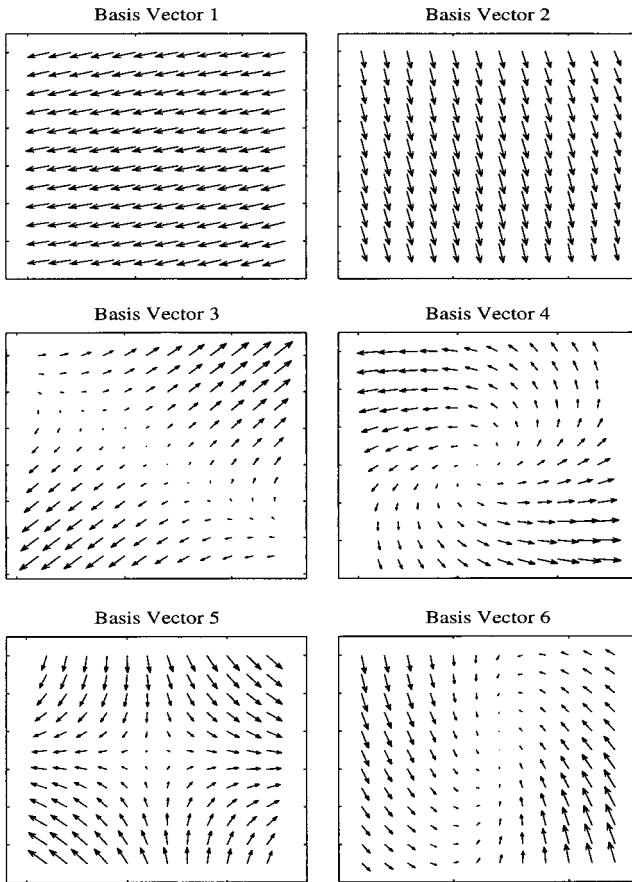


Figure 4. The first six basis vectors of the KL model.

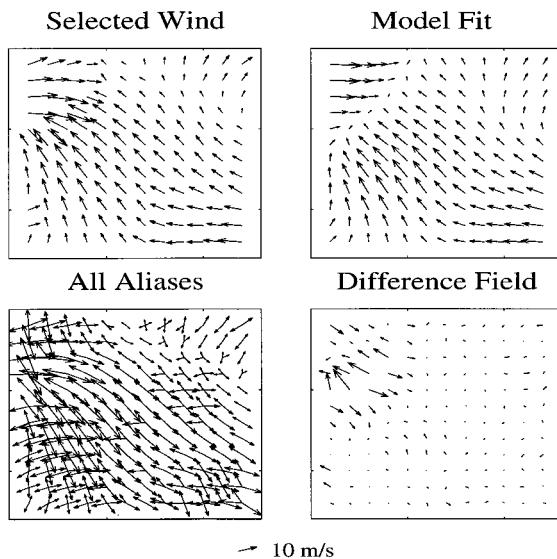


Figure 5. A wind field that exhibits a significant area of ambiguity removal errors in the upper left corner. The wind is spatially inconsistent in the upper left corner of the region, which is evident in the difference field, where large differences between the selected wind field and the model-fit field are observed. Because of the number of large values in the difference field, this region is classified as poor by the quality assurance (QA) algorithm.

pseudoinverse of \mathbf{F} , \mathbf{F}^\dagger ; that is, $\mathbf{X} = \mathbf{F}^\dagger \mathbf{W}_0$. The reconstructed wind field \mathbf{W}_R , also known as the model-fit field, is $\mathbf{W}_R = \mathbf{F}\mathbf{X}$, with the reconstruction difference field \mathbf{W}_E given by

$$\mathbf{W}_E = \mathbf{W}_R - \mathbf{W}_0 = (\mathbf{F}\mathbf{F}^\dagger - \mathbf{I})\mathbf{W}_0$$

If the reconstruction difference is small, then the model fit is good and the observed wind field is considered “realistic” according to the model. Large differences are attributed to possible ambiguity removal errors and flagged. However, the difference can also be affected by noise in the wind estimates or modeling error.

To illustrate, Figure 5 is a region with clear ambiguity removal errors in the upper left corner. The model-fit field exhibits large differences at some locations that correspond to the boundary of the ambiguity removal error region. By finding these areas of significant wind error in the model fit, ambiguity removal errors are identified.

There are a number of considerations when implementing this simple technique. First, the model must be fit to the wind field over a region. To produce an adequate fit, the input wind must be defined over the full region. Thus, for this simple algorithm, only those regions with fewer than eight cells of land or missing measurements are used. Since the reconstruction difference field becomes larger with increasing numbers of missing measurements, the threshold of eight cells was chosen as a conservative estimate. The missing measurements are replaced with the average of the cells surrounding it and then processed. Second, the wind field model inherently smoothes the wind field over the entire region owing to modeling error; the model matches the general flow of the wind but may not adequately model the center of a cyclone or the boundary of a front. Such regions can be flagged as containing errors, because the modeling error is large. Third, the difference in the model fit can be high in regions where the wind estimates are very noisy even if ambiguity removal is correct. Thus the region may be flagged as having possible ambiguity removal errors even if the ambiguity removal is correct. Fourth, it is possible for both the JPL field and the model-fit field to be incorrect for a given region, though it is impossible to detect this sort of occurrence with only NSCAT data. Finally, at low wind speeds the wind is highly variable, resulting in significant modeling error which is further complicated by the low signal-to-noise ratio in these regions. Manual ambiguity removal is also very difficult in such regions. As a result, we are unable to verify the ambiguity removal accuracy for low wind speed regions.

Figure 6 illustrates one such low wind speed region. Figure 7 demonstrates a region that is not represented well by the model fit. Neither of these regions is spatially consistent and

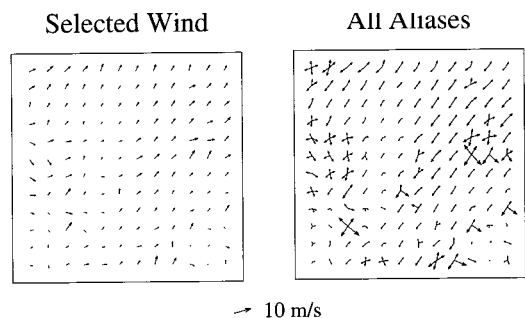


Figure 6. A region of low wind speed that is classified as poor by the QA algorithm.

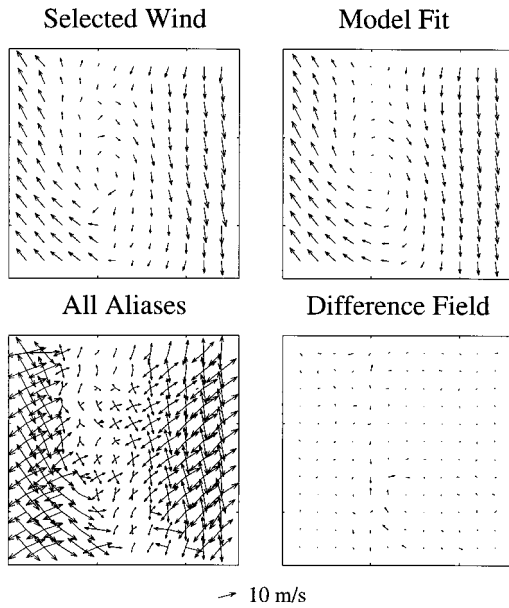


Figure 7. A region that is not represented well by the model fit and is flagged as poor.

results in large reconstruction differences. While the model fit seems to show the flow of the wind for this region, it is not clear that it is representative of the actual wind for this region. In such regions it can be difficult to verify the ambiguity removal accuracy because of the inherent uncertainty between modeling error and ambiguity removal error.

3.2. Selecting Thresholds

To use the model fit to locate regions with possible ambiguity removal errors, a set of thresholds on the model parameters and the reconstruction difference field are determined in the

following. These thresholds are used to classify the quality of the ambiguity removal for each region. A technique for correcting the identified errors is presented, and a description of the detection and correction algorithm is given.

To select the thresholds for the model parameters, a histogram of each parameter is examined. Figure 8 shows the histograms of four of the parameters for the KL model using 5488 regions of NSCAT data (6 days from 3 weeks). Experimental testing has shown that large values for any of the model parameters correspond to regions with possible errors. After some examination of the values for the parameters, the thresholds are set at twice the standard deviation for each of them. This provides an initial starting place for subjectively altering these numbers as needed to correctly identify error-prone regions. Only a few of the model parameters are necessary to identify regions of possible ambiguity removal errors. Since the columns of \mathbf{F} for the KL model are basis vectors in decreasing order, only the first few parameters are used as thresholds for the QA algorithm.

The other thresholds for locating ambiguity removal errors are determined from the reconstruction difference field. These thresholds include the rms error, the normalized rms error, the maximum component error, and the maximum direction error for each region. The rms error is found by summing the squared components of the reconstruction difference field, dividing by the number of terms, and taking the square root. The normalized rms error is found by squaring the components of the reconstruction difference field, dividing by the sum of the squared components of the observed wind field, and taking the square root, i.e., $n_{rms} = (\mathbf{W}_E^T \mathbf{W}_E / \mathbf{W}^T \mathbf{W})^{1/2}$. The rms and normalized rms errors aid in locating regions of large error. Both of these values are calculated for the entire region and thus provide information about the region as a whole. The maximum component and maximum direction error values are useful for locating regions in which only a few of the wind vectors

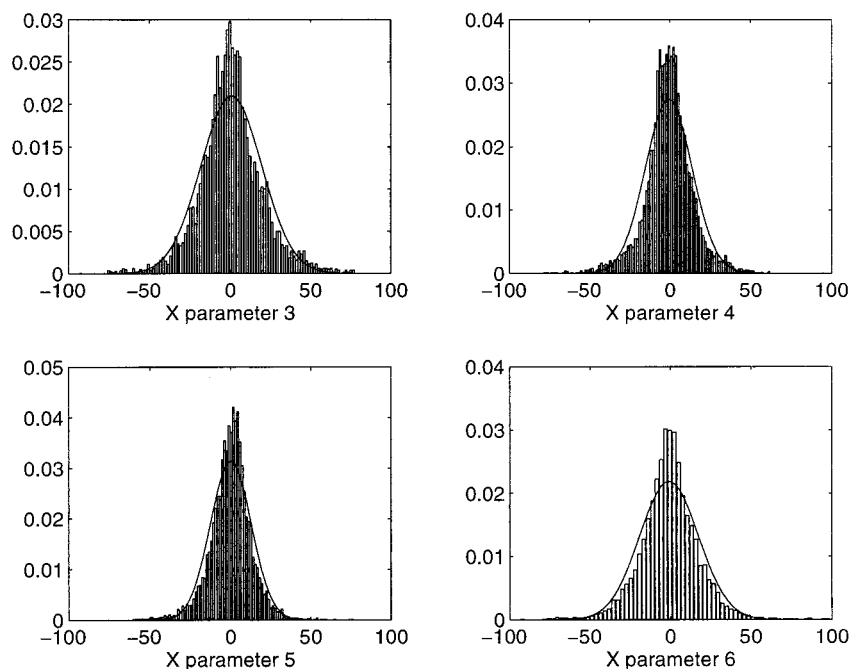


Figure 8. Histograms of estimated values for parameters 3 through 6 for the KL model. Overlaid is a Gaussian distribution with the same mean and variance.

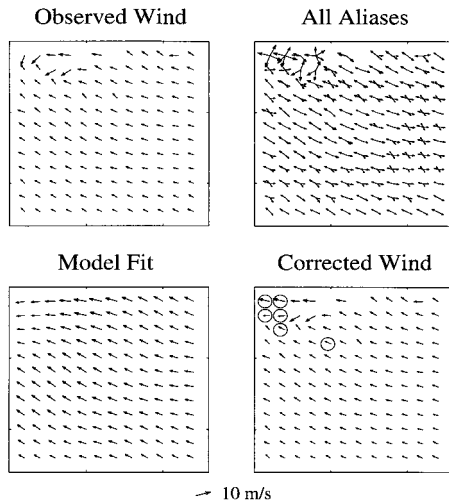


Figure 9. A sample corrected wind field. The circled vectors are those that were changed according to the method described in the text.

are incorrect. The individual errors are identified by finding those that exceed either of these thresholds. These wind vectors are flagged as possible ambiguity selection errors, though as discussed before, the error may exceed the thresholds owing to noise, modeling error, or ambiguity removal error.

To select the threshold values for this algorithm, 3309 regions (32 randomly selected revolutions) of NSCAT data were manually inspected. The regions were subjectively grouped into four categories: “perfect” (no errors), “good” (those with only a few isolated ambiguity removal errors), “moderate” (as much as 10% but less than 20% of the WVCs identified as possible ambiguity selection errors), and “poor” (more than 20% of WVCs identified as possible errors). All of the poor regions either have low rms wind speeds, making the region difficult to model, or have subjectively identified areas of significant ambiguity removal errors. While the possibility of a poor region classification due to modeling error exists, it was not observed in this data set. For this data set, 77% of the poor regions were low wind speed regions (rms speed less than a subjectively chosen threshold of 4 m s^{-1}). All of the remaining (with rms speed greater than 4 m s^{-1}) were regions with sub-

jectively identified areas of significant ambiguity removal errors. The statistics of each region were calculated and compared to the initial 2σ thresholds. The thresholds were adjusted such that the maximum number of poor, moderate, and good regions are correctly identified as containing ambiguity removal errors, with a minimum number of false alarms.

After this tuning, the algorithm correctly identified 100% of the poor and moderate regions and over 99% of the good regions with a false alarm rate of less than 3% on the tuning data set. Note that the thresholds can be altered to adjust the detection and false alarm probabilities since the thresholds are a tradeoff between detection and false alarms.

The thresholds chosen for the detection algorithm were tested on a manually classified withheld data set of 1561 regions (16 revolutions) and achieved a similar level of performance. The algorithm correctly identified 100% of the poor and moderate regions and over 98% of the good regions, with a false alarm rate of less than 4%. Combining the statistics for these two data sets results in a total detection rate of more than 98% for all regions subjectively identified as containing ambiguity removal errors, with less than 4% of the perfect regions misidentified. Thus, though modeling error or noise will sometimes result in an incorrect evaluation of a region as containing possible errors, the vast majority of regions with possible ambiguity removal errors are located using this technique. The classification performance of low wind speed regions was also consistent with the previous results. Regions with low ($<4 \text{ m s}^{-1}$) rms wind speeds accounted for 76% of the poor regions, with the remaining regions (with rms wind speeds greater than 4 m s^{-1}) all containing significant areas of ambiguity removal errors.

Regions with possible errors are then tested for consideration in the correction algorithm in which wind vectors are examined individually. For vectors identified as possible ambiguity removal errors, the pointwise ambiguity closest in direction to the model fit is chosen as the corrected wind. Since the ambiguities typically have similar speeds but different directions, the speed field remains similar, but the direction field is more consistent with the model fit for corrected wind fields. Figure 9 demonstrates the use of the correction algorithm. As can be seen, the observed wind product contains several ambiguity removal errors. The algorithm chooses the ambiguity that is closest in direction to the model-fit field, producing a

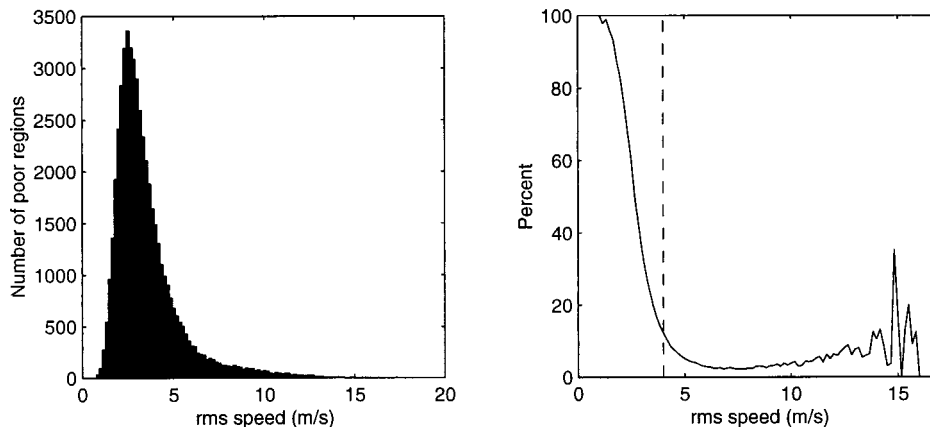


Figure 10. (left) Histogram of the rms speed for all regions classified as “poor” in the 9-months NASA scatterometer (NSCAT) mission. (right) Percent of the total regions that are classified as poor at each rms wind speed bin. The vertical dashed line is at 4 m s^{-1} .

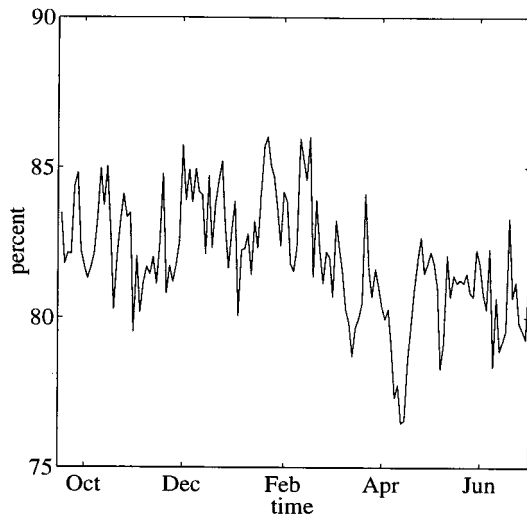


Figure 11. Percent of nonpoor regions versus time over the 9-month NSCAT mission. Each point represents the average computed over approximately 2 days.

subjectively more realistic corrected wind field. Thus the model fit is a reasonable basis for both detecting ambiguity removal errors and correcting at least some ambiguity removal errors.

However, as mentioned, the model does not adequately fit some wind fields, or as a result of significant ambiguity errors, the original wind field cannot be determined with confidence using the model. Thus the model-fit field cannot be used to attempt to correct these wind fields. The number of possible ambiguity removal errors is used as a criterion for determining when a region is a candidate for the correction algorithm. The number of possible ambiguity removal errors, i.e., the number of WVCs flagged by the QA algorithm as having large differences with the model, is determined by those wind vectors that exceed either the maximum direction or maximum component error thresholds. If the total number of errors for a region

exceeds this threshold, the region is not considered a candidate for the correction algorithm. The selection of the threshold was determined by trial and error. For this implementation, only regions classified as good or moderate (i.e., with 20% or fewer possible errors) are considered candidates for ambiguity selection correction.

The criteria for an ambiguity removal correction of a WVC is thus extremely conservative. Further, though the vector may be identified as being potentially in error (due, perhaps, to a noisy wind vector estimate), many times, the ambiguity closest in direction to the model fit is, in fact, the original wind vector and thus no change is made. For example, in Figure 9, even after attempted correction, a few of the wind vectors still appear quite noisy and, as a result, are still flagged by the algorithm as possibly incorrect even though no better directional ambiguity can be found.

4. Analysis

After the algorithm was tuned with 10 revolutions of NSCAT data, the entire 9-month nudged NSCAT mission data set was processed to assess the accuracy of NSCAT ambiguity removal. The results were consistent with the results already presented herein for the observation subset used to develop the model. Of 408,069 regions examined, 24% were classified as perfect 41% as good, 17% as moderate, and 18% as poor, according to the categories described in section 3.2.

For regions classified as perfect, good, or moderate (82% of the total), only 4% of the individual vectors were identified as possible ambiguity removal errors; however, only approximately 10% of these vectors were changed using the model-based correction technique. For the remaining, the ambiguity closest in direction to the model fit was the original wind vector. Thus only 0.4% of the individual vectors were corrected using this approach. This result suggests that NSCAT ambiguity removal is thus over 99% effective for these regions.

Figure 10 summarizes key statistics for regions (18% of the total) classified as poor. Of these poor regions, 74% of them

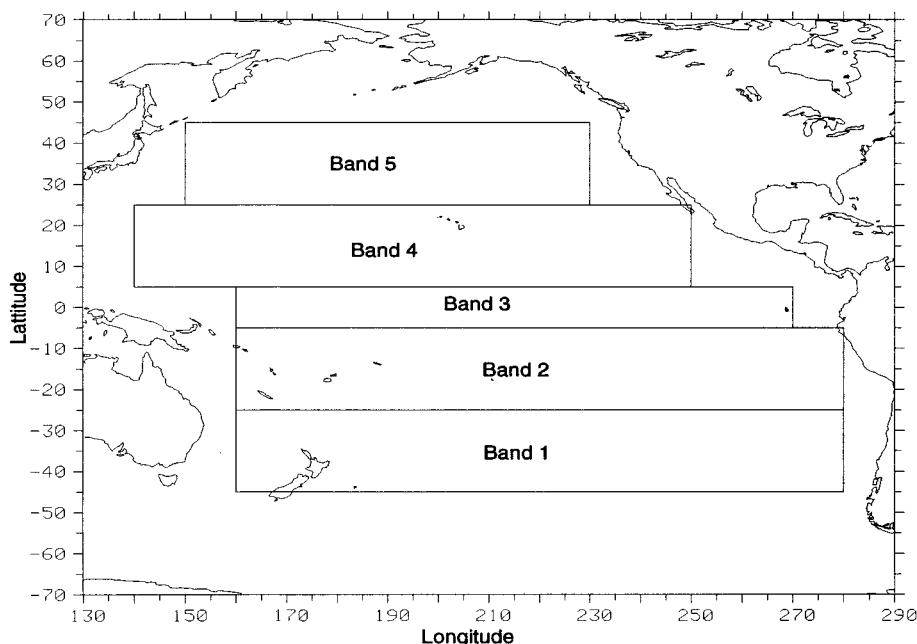


Figure 12. Geographical latitude bands in the Pacific.

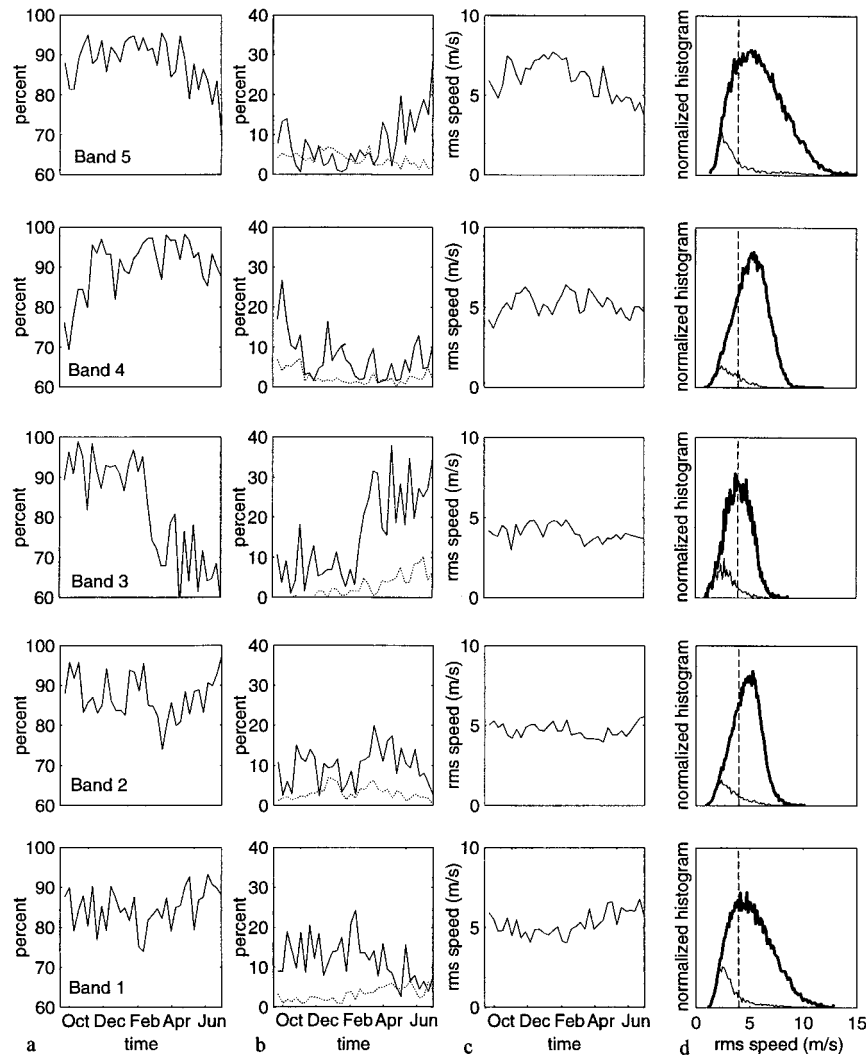


Figure 13. (a) Percentage of nonpoor regions as a function of time over the NSCAT mission. (b) Percentage of poor regions with an rms wind speed greater than (solid curve) and less than (dotted curve) 4 m s^{-1} . (c) Average regional rms wind speed as a function of time. (d) Normalized histograms of all regions (thick curve) and those classified as poor by the QA algorithm (thin curve). The vertical dashed line is a 4 m s^{-1} .

have rms speed values of 4 m s^{-1} or less, and we are unable to verify the ambiguity removal accuracy owing to the difficulty of modeling low wind speed regions and the noise level at low wind speeds. The poor regions with rms wind speeds greater than 4 m s^{-1} contain significant ambiguity removal errors. Such regions represent less than 5% of the total number of regions. We note from Figure 10 that not all regions with rms wind speeds less than 4 m s^{-1} are rated poor but that all regions with an rms wind speed less than approximately 2 m s^{-1} are rated poor. This is consistent with a low wind speed cutoff in the geophysical model function such as that proposed by *Donelan and Pierson* [1987], who suggested that below a temperature-dependent wind speed threshold of 3 to 5 m s^{-1} at Ku band, depending on incidence angle, the normalized radar cross section falls off rapidly. Such a roll-off would decrease the signal-to-noise ratio and reduce the accuracy of the wind estimates.

Although 5% of the total number of regions have large ambiguity removal errors, portions of these regions contain no errors. Since we cannot uniquely resolve corrections using only

NSCAT data and this simple technique for these high wind speed ($>4 \text{ m s}^{-1}$) poor regions, a conservative approach is to treat each wind vector in the region as a possible ambiguity removal error. Combining this with the previous result of almost complete effectiveness for nonpoor regions, we conservatively conclude that, based only on NSCAT data, the effectiveness of NSCAT ambiguity removal is 95% or better for the entire set of regions with rms wind speeds of 4 m s^{-1} or greater.

The accuracy of NSCAT ambiguity removal is evaluated as a function of time during the mission in Figure 11, which shows the percent of nonpoor regions as a function of time. There is an apparent slight decrease in the accuracy of NSCAT ambiguity removal over the mission. To understand this effect, the ambiguity removal is evaluated over several Pacific Ocean latitude bands as defined in Figure 12. Figure 13 summarizes some of the statistics over the five latitude bands. The expected variation of wind speed with latitude is clearly evident. There is a strong correlation between the ambiguity removal performance and the rms wind speed, with reduced overall ambiguity

removal performance (i.e., more poor regions) at lower wind speeds. Thus the wind speed distribution in each band affects the ambiguity removal performances, and seasonal changes in the wind speed distribution results in temporal variations in the ambiguity removal performance. In particular, increased storm activity in the northern hemisphere results in increased wind speed with improved ambiguity removal during the winter months in bands 4 and 5. Similarly, the number of poor regions increases during the southern hemisphere summer owing to a decrease in the rms wind speed. The peak in the percentage of high wind speed poor regions in band 1 corresponds to early winter in the southern hemisphere, a time of large storms in this region. Because of its low rms wind speed, equatorial band 3 is the most sensitive to changes in the mean rms wind speed, with a significant drop in the percent of nonpoor regions corresponding to a small drop in the rms wind speed at the start of 1997.

5. Summary and Conclusions

In summary, the steps of the algorithm to detect and correct ambiguity removal errors are the following.

1. Segment the swath into 12×12 overlapping regions with 50% along track (6 WVCs) overlap.
2. For each valid region (regions with fewer than eight missing measurements or land cells), compute the model-fit field \mathbf{W} , the reconstruction error field \mathbf{W}_E , the model parameter vector \mathbf{X} , and the statistics of \mathbf{W}_E . These statistics include the rms error, the normalized rms error, the maximum component error, and the maximum direction error for each region.
3. For each region, determine if the statistics, including those for the model parameter vector \mathbf{X} , are larger than the thresholds. If so, the region is identified as containing possible ambiguity selection errors. On the basis of the number of possible errors identified for each region, segregate the regions into four classes (perfect, good, moderate, and poor).
4. For those regions not classified as poor, correct the ambiguity removal error by choosing the ambiguity closest in direction to the model fit for those WVCs identified as possible errors.

In conclusion, using only NSCAT data, the QA algorithm works very well in identifying regions with possible selection errors. The technique allows rapid processing of the data set. Ambiguity removal errors in good or moderate regions can be corrected with a high degree of confidence. Using this technique over the 9-month NSCAT mission, the NSCAT ambiguity removal is found to be better than 95% effective for the entire set of regions with rms wind speeds greater than 4 m s^{-1} .

Acknowledgments. This work was completed at the Brigham Young University Microwave Earth Remote Sensing Laboratory and was supported by the National Aeronautic and Space Administration. NSCAT data were obtained from the PODAAC at the Jet Propulsion Laboratory. We would also like to thank Stephen Richards for his help in producing these results.

References

- Atlas, R., A. J. Busalaci, M. Ghil, S. Bloom, and E. Kalnay, Global surface wind flux fields from model assimilation of Seasat data, *J. Geophys. Res.*, 92, 6477–6487, 1987.
- Donelan, M., and W. Pierson, Radax scattering and equilibrium ranges in wind-generated waves with application to scatterometry, *J. Geophys. Res.*, 92, 4971–5029, 1987.
- Freilich, M. H., and R. S. Dunbar, The accuracy of the NSCAT 1 vector winds: Comparisons with National Data Buoy Center buoys, *J. Geophys. Res.*, this issue.
- Gunther, J., and D. G. Long, Models of the near-surface oceanic vorticity and divergences, paper presented at International Geoscience and Remote Sensing Symposium, Inst. of Electr. and Electron Eng., New York, 1994.
- Hoffman, R. N., SASS wind ambiguity removal by direct minimization, *Mon. Weather Rev.*, 110, 434–445, 1982.
- Long, D. G., Wind field model-based estimation of Seasat scatterometer winds, *J. Geophys. Res.*, 98, 14,651–14,688, 1993.
- Long, D. G., and J. M. Mendel, Identifiability in wind estimation from scatterometer measurements, *IEEE Trans. Geosci. Remote Sens.*, 29, 268–276, 1991.
- Naderi, F., M. Freilich, and D. G. Long, Spaceborne radar measurement of wind velocity over the ocean—An overview of the NSCAT scatterometer system, *Proc. IEEE*, 79(6), 850–866, 1991.
- Oliphant, T. E., New techniques for wind scatterometry, M.S. thesis, 168 pp., Brigham Young Univ., Provo, Utah, Aug. 1996.
- Schroeder, L. C., W. L. Grantham, E. M. Bracalente, C. L. Britt, K. S. Shanmugam, F. J. Wentz, D. P. Wyle, and B. B. Hinton, Removal of ambiguous wind directions for a Ku-band wind scatterometer using measurements at three different azimuth angles, *IEEE Trans. Geosci. Remote Sens.*, GE-23, 91–100, 1985.
- Shaffer, S. J., R. S. Dunbar, S. V. Hsiao, and D. G. Long, A median-filter-based ambiguity removal algorithm for NSCAT, *IEEE Trans. Geosci. Remote Sens.*, 29, 167–174, 1991.
- Shultz, H., A circular median filter for resolving directional ambiguities retrieved from spaceborne scatterometer data, *J. Geophys. Res.*, 95, 5291–5303, 1990.
- Wentz, F., and D. Smith, A model function for the ocean-normalized radar cross section at 14.6 GHz derived from NSCAT observations, *J. Geophys. Res.*, this issue.

A. E. Gonzales and D. G. Long, Department of Electrical and Computer Engineering, Brigham Young University, 459 Clyde Building, Provo, UT 84604. (e-mail: gonzalae@ee.byu.edu; long@ee.byu.edu)

(Received March 4, 1998; revised May 19, 1998; accepted June 5, 1998.)

